MRR OPTIMIZATION IN NANO-MQL MILLING OF HARDENED 90CRSI TOOL STEEL USING CUO NANOPARTICLES

TỐI ƯU HÓA TỐC ĐỘ BÓC TÁCH VẬT LIỆU TRONG QUÁ TRÌNH PHAY THÉP 90CRSI TÔI CỨNG SỬ DỤNG BÔI TRƠN NANO-MQL VỚI HẠT CUO

Luu Anh Tung[1], Hoang Van Got[2], Do The Vinh[1], Vu Ngoc Pi[1], Hoang Anh Toan[1,*]
[1]Thai Nguyen University of Technology, Thai Nguyen city, Vietnam
[2]National Research Institute of Mechanical Engineering, Hanoi city, Vietnam
Corresponding author: hoanganhtoan@tnut.edu.vn

ABSTRACT

This study aims to optimize the material removal rate (MRR) in the hard milling of 90CrSi tool steel under nano-minimum quantity lubrication (Nano-MQL) conditions. A Box–Behnken Design (BBD) was employed to investigate the effects of cutting speed, feed per tooth, depth of cut, and CuO nanoparticle size on MRR. A total of 45 experiments were conducted using a nano-composite coated carbide tool (Ø12 mm, 6 flutes) on hardened 90CrSi steel with a hardness of 56-60 HRC. The nano-lubricant was prepared by dispersing 2 wt.% CuO nanoparticles into canola oil and delivered to the cutting zone at a flow rate of 100 mL/h with a compressed air pressure of 4 atm. A second-order regression model was developed to analyze the influence of each factor and their interactions on MRR. Main effects plots and surface response analysis were also performed to visualize trends and identify optimal conditions. The results showed that cutting speed and depth of cut were the most significant contributors to MRR, while CuO nanoparticle size had a secondary but positive effect. The regression model demonstrated high predictive accuracy, providing a valuable tool for parameter selection in sustainable machining of hard materials.

Keywords: *Material removal rate (MRR); Nano-MQL CuO nanoparticles; Hard milling; 90CrSi tool steel; Box–Behnken Design; Process optimization.*

TÓM TẮT

Nghiên cứu này nhằm tối ưu hóa tốc độ bóc tách vật liệu (MRR) trong quá trình phay thép dụng cụ 90CrSi đã tôi cứng, sử dụng phương pháp bôi trơn tối thiểu có pha hạt nano (Nano-MQL). Thiết kế thí nghiệm Box–Behnken (BBD) được sử dụng để khảo sát ảnh hưởng của tốc độ cắt, lượng chạy dao trên mỗi răng, chiều sâu cắt và kích thước hạt CuO đến MRR. Tổng cộng 45 thí nghiệm đã được thực hiện sử dụng dao phay hợp kim phủ nano-composite (Ø12 mm, 6 me cắt) trên vật liệu 90CrSi có độ cứng 56-60 HRC. Dung dịch bôi trơn nano được pha chế bằng cách phân tán 2% khối lượng hạt CuO trong dầu hạt cải, và được cung cấp đến vùng cắt với lưu lượng 100 mL/h dưới áp suất khí nén 4 at. Mô hình hồi quy bậc hai được xây dựng nhằm phân tích mức độ ảnh hưởng của từng yếu tố cũng như các tương tác giữa chúng đến MRR. Đồng thời, các biểu đồ hiệu ứng chính và phân tích bề mặt đáp ứng cũng được thực hiện để minh họa xu hướng và xác định điều kiện tối ưu.

Kết quả cho thấy tốc độ cắt và chiều sâu cắt là hai yếu tố ảnh hưởng lớn nhất đến MRR, trong khi kích thước hạt CuO có ảnh hưởng thứ yếu nhưng tích cực. Mô hình hồi quy thu được có độ chính xác cao, là công cụ hữu ích trong việc lựa chọn thông số công nghệ phù hợp nhằm nâng cao hiệu quả gia công bền vững vật liệu cứng.

Từ khóa: *Tốc độ bóc tách vật liệu (MRR); Nano-MQL; Hạt nano CuO; Phay cứng; Thép dụng cụ 90CrSi; Thiết kế Box–Behnken; Tối ưu hóa thông số gia công.*

1. INTRODUCTION

Material removal rate (MRR) is a fundamental indicator of machining productivity, particularly in hard milling processes where tool wear, surface integrity, and machining stability are tightly coupled. With the increasing demand for sustainable and high-efficiency manufacturing, enhancing MRR without compromising tool life and surface quality has become a critical research objective.

Tool damage and coating failure are primary factors influencing MRR. Gutnichenko et al. [1] studied the early-stage damage of TiAlN-coated PcBN tools in hard milling of Vanadis 4E steel and emphasized how coating failure significantly affects tool efficiency. In a related study, Hassanpour et al. [2] found that flank wear in ball nose tools reduces both surface integrity and removal efficiency, even under MQL conditions.

The material response under cutting loads has also been explored. Vovk et al. [3] conducted numerical simulations to examine how multi-axis loading alters subsurface material characteristics in hard milling, providing insights into chip formation and removal rates. Similarly, Zhang et al. [4] used finite element modeling to simulate cutting forces and temperature, confirming that high thermal loads can hinder effective material removal.

Energy efficiency and MRR have shown strong interdependence. Liu et al. [5] characterized energy consumption patterns in finish hard milling and concluded that optimal removal rates align with minimal energy waste. Building on this, Khare et al. [6] demonstrated experimentally that increasing cutting speed directly improves MRR in face milling.

Tool conditioning and cooling methods are also crucial. Li et al. [7] revealed that deep cryogenic treatment of carbide tools improved their wear resistance, leading to enhanced MRR in hard milling of AISI H13 steel. Coating strategies were examined by Beake et al. [8], who compared different PVD coatings in wet milling and found that thermal-stable coatings extend tool life and increase MRR.

Several researchers have utilized modeling and optimization techniques to predict and enhance MRR. Jenarthanan and Neeli [9] employed grey relational analysis (GRA) to optimize parameters affecting MRR in milling of GFRP composites, while MP et al. [10] confirmed that end milling MRR can be maximized using multi-objective GRA. In hard milling of AISI 4340, Hassanpour et al. [11] showed that applying MQL not only reduced tool wear and thermal damage but also improved chip evacuation and material removal.

The role of advanced coatings and tool design has been further explored. Bian et al. [12] ☞

investigated meso-scale hard milling of zirconia using diamond-coated tools, achieving significant improvements in MRR under optimized conditions. An et al. [13] found that PVD-AlTiN coated carbide tools maintained high MRR when machining high-strength steel, confirming the importance of tool–coating compatibility.

Liu et al. [14] analyzed tool wear progression and its effect on energy consumption and MRR, emphasizing the value of real-time monitoring for sustainable process control. The cumulative effect of residual stresses in coated tools was highlighted by Teppernegg et al. [15], [16], who reported that long-term stress accumulation affects tool stability and removal rate under hard cutting conditions.

Recent studies have extended MRR optimization to lightweight alloys. Jayakumar and Rahman [17] studied AA7075 and found that optimized end milling parameters simultaneously improved MRR and mechanical properties. Tamilarasan et al. [18] applied fuzzy logic and regression modeling in hard milling to accurately predict MRR under varying cutting environments.

While these studies have contributed significantly to MRR enhancement, limited work has focused on the synergistic effects of Nano-MQL and nanoparticle characteristics especially CuO nanoparticles on MRR in hard milling of high-hardness steels. This study addresses this gap by experimentally analyzing and modeling the influence of cutting parameters and CuO nanoparticle size on MRR during the Nano-MQL milling of hardened 90CrSi steel. A Box–Behnken Design (BBD) is used to efficiently explore process parameter interactions and optimize material removal under sustainable conditions.

2. EXPERIMENTAL WORK

2.1. Experimental Design

A Box–Behnken Design (BBD) was employed to investigate the effect of key cutting parameters and nano-lubrication conditions on the Material Removal Rate (MRR) during hard milling. The BBD approach was selected due to its efficiency in modeling quadratic relationships with fewer runs compared to a full factorial design, while still enabling the analysis of factor interactions.

Four independent input variables were selected: cutting speed (v_c), feed per tooth (f_z), axial depth of cut (a_p), and average nanoparticle size (D_{avg}). Each variable was set at three levels, as shown in Table 1.

Table 1. Input parameters and levels used in Box–Behnken Design

Factor	Symbol	Unit	Level −1	Level 0	Level +1
Cutting speed	v_c	m/min	100	125	150
Feed per tooth	f_z	mm/tooth	0.04	0.06	0.08
Depth of cut	a_p	mm	0.10	0.15	0.20
Nanoparticle size	D_{avg}	nm	20	50	100

Based on the BBD matrix for four factors at three levels, a total of 45 experiments were conducted. The complete experimental matrix and corresponding MRR results are provided in Table 2.

Table 2. Experimental matrix and output results

Trial.	v_c (m/min.)	f_z (mm/tooth)	a_p (mm)	D_{avg} (nm)	MRR
1	150	0.06	0.2	20	1433.121
2	150	0.04	0.15	100	716.5605
3	125	0.06	0.15	100	895.7006
4	150	0.06	0.15	50	1074.841
5	150	0.08	0.2	50	1910.828
6	100	0.06	0.25	20	1194.268
7	125	0.06	0.2	100	1194.268
8	100	0.04	0.15	100	477.707
9	150	0.06	0.15	100	1074.841
10	150	0.06	0.25	100	1791.401
11	125	0.08	0.15	50	1194.268
12	100	0.06	0.2	20	955.414
13	150	0.04	0.15	50	716.5605
14	125	0.06	0.15	100	895.7006
15	125	0.06	0.25	20	1492.834
16	125	0.08	0.2	50	1592.357
17	100	0.04	0.15	20	477.707
18	150	0.06	0.2	20	1433.121
19	125	0.08	0.25	100	1990.446
20	100	0.08	0.15	100	955.414
21	125	0.06	0.15	50	895.7006
22	150	0.08	0.25	20	2388.535
23	125	0.08	0.2	20	1592.357
24	100	0.06	0.25	50	1194.268
25	125	0.08	0.15	20	1194.268
26	125	0.04	0.2	100	796.1783
27	125	0.04	0.25	100	995.2229
28	100	0.04	0.2	50	636.9427
29	125	0.04	0.15	20	597.1338
30	125	0.04	0.25	50	995.2229
31	100	0.06	0.15	100	716.5605
32	100	0.06	0.2	100	955.414

33	150	0.06	0.25	50	1791.401
34	125	0.06	0.2	50	1194.268
35	125	0.06	0.15	20	895.7006
36	150	0.08	0.15	100	1433.121
37	125	0.08	0.15	100	1194.268
38	100	0.06	0.15	50	716.5605
39	100	0.08	0.2	50	1273.885
40	100	0.08	0.25	20	1592.357
41	125	0.04	0.2	20	796.1783
42	125	0.06	0.15	20	895.7006
43	150	0.04	0.15	20	716.5605
44	100	0.04	0.15	50	477.707
45	100	0.08	0.25	50	1592.357

2.2. Experimental Setup

All experiments were performed on a vertical CNC machining center. The workpiece material used was 90CrSi tool steel, which was heat-treated to achieve a hardness of 56-60 HRC, making it suitable for hard milling research. The cutting tool employed in all trials was a nano-composite coated solid carbide end mill (model CEPR6120-TH, Ø12 mm, 6 flutes). A Nano-MQL system was implemented for lubrication, utilizing a mixture of canola oil and 2 wt.% CuO nanoparticles, delivered at a flow rate of 100 mL/h using compressed air at 4 atm.

The experimental configuration is illustrated in Figure 1, showing the workpiece clamping, tool holder, Nano-MQL nozzle orientation, and the data collection devices.

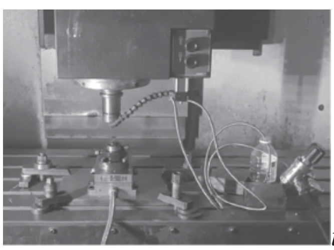

Figure 1. Experimental setup

2.3. Material Removal Rate Calculation

The Material Removal Rate (MRR) was calculated for each experiment based on the process parameters using the volumetric formulation shown in Equation (1):

$$MRR = v_c \cdot f_z \cdot a_p \cdot z \qquad (1)$$

Where v_c is the cutting speed (m/min), f_z is the feed per tooth (mm/tooth), a_p is the depth of cut (mm), and z = 6 is the number of tool flutes (cutting edges).

3. RESULTS AND DISCUSSION

3.1. Regression Model of MRR

A second-order polynomial regression model was developed to predict Material Removal Rate (MRR) as a function of cutting parameters and CuO nanoparticle size. The regression equation is given below:

$$\begin{aligned} MRR = {} & 0.5274\,D_{avg} - 5911.0\,a_p - 17540.0\,f_z \\ & - 8.527\,v_c - 0.6172\,D_{avg}a_p + 0.4884\,D_{avg}f_z \\ & - 0.003809\,D_{avg}v_c + 97590.0\,a_pf_z + 49.79\,a_pv_c + 141.5\,f_zv_c \\ & + 0.0001939\,D_{avg}^2 - 413.7\,a_p^2 + 938.1\,f_z^2 + 0.0003428\,v_c^2 + 1028.0 \end{aligned} \qquad (1)$$

The model achieved an exceptionally high coefficient of determination $R^2 = 0.9996$, indicating near-perfect agreement between experimental and predicted MRR values. As shown in Figure 2, the data points fall closely along the 45° reference line, confirming the accuracy and reliability of the model.

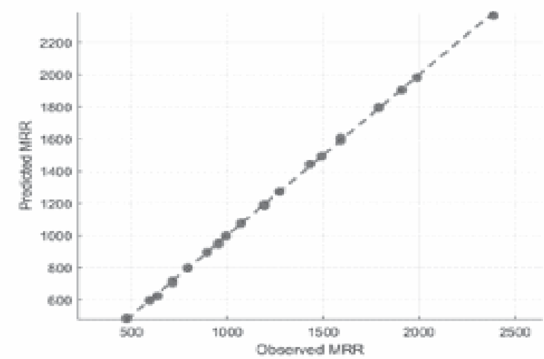

Figure 2. Regression plot

3.2. Influence of Individual Parameters

The relative importance of each factor was assessed using standardized regression coefficients, as depicted in Figure 3. The analysis reveals that:

- Feed per tooth (f_z) is the most dominant factor influencing MRR, followed closely by depth of cut (apa_pap) and cutting speed (v_c).

- The nanoparticle size (D_{avg}) has a noticeably smaller effect on MRR compared to geometric and kinematic parameters.

- Quadratic and interaction terms also contribute, but to a lesser extent than the main linear effects.

These findings are consistent with the physical understanding of MRR, which is directly proportional to the product of v_c, f_z and a_p as seen in Equation (1).

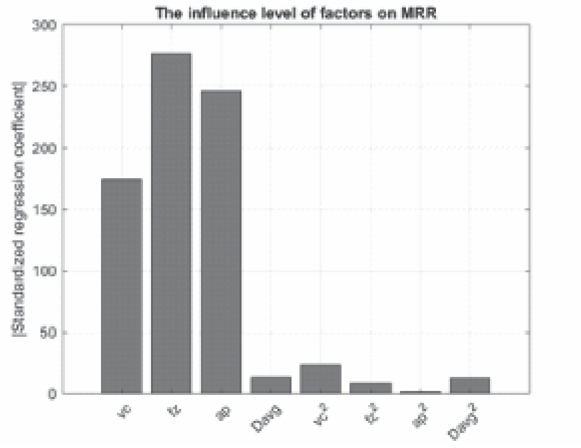

Figure 3. The standardized regression coefficients

3.3. Main Effects Analysis

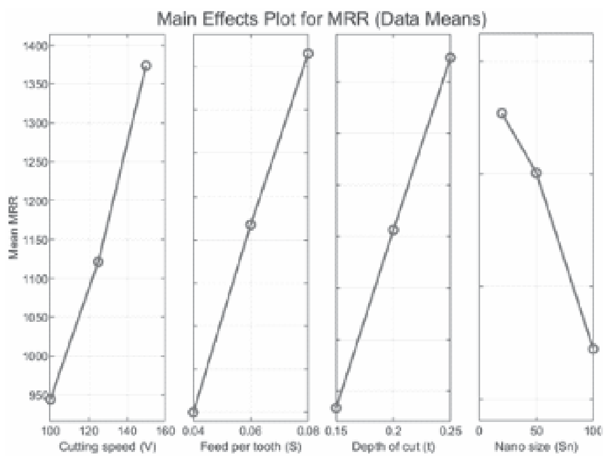

Figure 4. Main effects plot for MRR

The main effects plot for MRR is shown in Figure 4. It illustrates the average MRR response across each level of the four input parameters:

- MRR increases significantly with higher cutting speed, feed per tooth, and depth of cut, as expected from the volumetric definition.

- Interestingly, increasing CuO nanoparticle size from 20 to 100 nm leads to a slight decrease in MRR. This may be attributed ☞

to increased viscosity or reduced atomization efficiency at higher particle sizes, which could affect chip evacuation and cutting force.

3.4. Surface and Contour Plot Analysis

The combined effect of feed per tooth (f_z) and nanoparticle size (D_{avg}) on MRR was visualized using contour and surface plots in Figures 5 and 6, respectively.

- Both plots show that MRR increases strongly with feed per tooth, while the influence of nanoparticle size is more moderate.

- At lower f_z, the impact of D_{avg} on MRR is negligible, but becomes more noticeable as f_z increases.

- The surface plot shows a smooth, continuously rising response along the f_z direction, reinforcing the conclusion that feed rate is the key driver of MRR in this process.

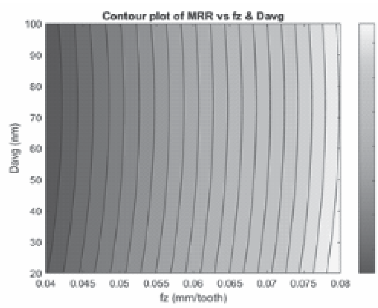

Figure 5. Contour plot for MRR

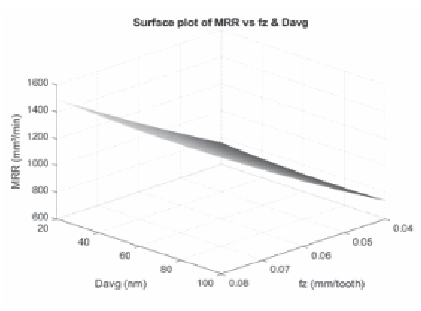

Figure 6. Surface plot for MRR

3.5. Summary of Findings

- The developed regression model for MRR shows excellent predictive capability with $R^2 = 0.9996$.

- Feed per tooth is the most influential factor, followed by depth of cut and cutting speed.

- Larger nanoparticle sizes tend to slightly reduce MRR, suggesting a trade-off between cooling/lubrication performance and material removal efficiency.

- The findings support the use of CuO-based Nano-MQL as a viable strategy for sustainable, high-efficiency hard milling.

4. CONCLUSION

This study focused on the modeling and optimization of MRR during the hard milling of 90CrSi tool steel using a CuO-based Nano-MQL lubrication system. A total of 45 experiments were conducted based on a Box–Behnken Design, considering four key input parameters: cutting speed, feed per tooth, depth of cut, and nanoparticle size.

- A second-order regression model was successfully developed to predict MRR with very high accuracy ($R^2 = 0.9996$). The analysis of standardized regression coefficients, main effects plots, and surface/contour graphs led to the following conclusions:

- Feed per tooth (f_z) is the most dominant factor influencing MRR, followed closely by depth of cut (a_p) and cutting speed (v_c).

- Nanoparticle size (D_{avg}) showed a moderate inverse influence on MRR, particularly at higher feed rates.

- The regression model closely matched experimental data, as evidenced by a tight clustering of predicted vs. observed values.
- The combined use of CuO nanoparticles and canola oil in the Nano-MQL setup enabled stable and sustainable machining with high removal efficiency.

Overall, the results demonstrate that CuO-based Nano-MQL lubrication is an effective approach to enhance MRR in the hard milling of 90CrSi steel, and the proposed model provides a reliable basis for parameter selection and process optimization in sustainable machining applications.

Acknowledgment:

This work was supported by Thai Nguyen University of Technology (TNUT).❖

References:

[1]. O. Gutnichenko, S. G. Pozuelo, L. Llanes, and V. Bushlya, “*Analysis and Monitoring the Initial Tool Damage and Coating Failure when Hard Milling Vanadis 4E with TiAlN Coated PcBN*”. Procedia CIRP, vol. 133, pp. 322-327, 2025.

[2]. H. Hassanpour, A. Rasti, J. H. Khosrowshahi, and S. S. Farshi, “*Effect of ball nose flank wear on surface integrity in high-speed hard milling of AISI 4340 steel using MQ*L”. Heliyon, vol. 10, no. 18, 2024.

[3]. A. Vovk, J. Sölter, and B. Karpuschewski, “*Numerical investigation of the influence of multiple loads on material modifications during hard milling*”. Procedia CIRP, vol. 102, pp. 500-505, 2021.

[4]. Q. Zhang, S. Zhang, and J. Li, “*Three dimensional finite element simulation of cutting forces and cutting temperature in hard milling of AISI H13 steel*”. Procedia Manufacturing, vol. 10, pp. 37-47, 2017.

[5]. Z. Liu et al., “*Energy consumption characteristics in finish hard milling*”. Journal of Manufacturing Processes, vol. 35, pp. 500-507, 2018.

[6]. S. K. Khare, P. Gulati, and J. P. Singh, “*Enhancing MRR in face milling by varying cutting speed*”. Materials Today: Proceedings, 2023.

[7]. B. Li, T. Zhang, and S. Zhang, “*Deep cryogenic treatment of carbide tool and its cutting performances in hard milling of AISI H13 steel*”. Procedia CIRP, vol. 71, pp. 35-40, 2018.

[8]. B. Beake et al., “*Wear performance of different PVD coatings during hard wet end milling of H13 tool stee*l”. Surface and Coatings Technology, vol. 279, pp. 118-125, 2015.

[9]. M. Jenarthanan and N. Neeli, “*Optimization of process parameters on machining force and MRR in milling of GFRP composites using grey relational analysis*”. i-Manager's Journal on Material Science, vol. 1, no. 3, p. 29, 2013.

[10]. J. MP, P. K. R. Gavireddy, C. S. Gummadi, and S. R. Mandapaka, “*Optimization of process parameters on machining force and MRR during end milling of GFRP composites using GR*A”. World Journal of Engineering, vol. 15, no. 3, pp. 407-413, 2018.

[11]. H. Hassanpour, M. H. Sadeghi, A. Rasti, and S. Shajari, “*Investigation of surface roughness, microhardness and white layer thickness in hard milling of AISI 4340 using minimum quantity lubrication*”. Journal of Cleaner Production, vol. 120, pp. 124-134, 2016.

[12]. R. Bian, E. Ferraris, N. He, and D. Reynaerts, “*Process investigation on meso-scale hard milling of ZrO_2 by diamond coated tools*”. Precision Engineering, vol. 38, no. 1, pp. 82-91, 2014.

[13]. Q. An, C. Wang, J. Xu, P. Liu, and M. Chen, “*Experimental investigation on hard milling of high strength steel using PVD-AlTiN coated cemented carbide tool*”. International Journal of Refractory Metals and Hard Materials, vol. 43, pp. 94-101, 2014.

[14]. Z. Liu, Y. Guo, M. Sealy, and Z. Liu, “*Energy consumption and process sustainability of hard milling with tool wear progression*”. Journal of Materials Processing Technology, vol. 229, pp. 305-312, 2016.

[15]. T. Teppernegg et al., “*Evolution of residual stress and damage in coated hard metal milling inserts over the complete tool life*”. International Journal of Refractory Metals and Hard Materials, vol. 47, pp. 80-85, 2014.

[16]. T. Teppernegg, P. Angerer, T. Klünsner, C. Tritremmel, and C. Czettl, “*Evolution of residual stress in Ti-Al-Ta-N coatings on hard metal milling inserts*”. International Journal of Refractory Metals and Hard Materials, vol. 52, pp. 171-175, 2015.

[17]. K. Jayakumar and P. A. Rahman, “*Effect of end milling parameters on MRR and hardness variation of AA7075*”. Materials Today: Proceedings, vol. 72, pp. 2212-2216, 2023.

[18] A. Tamilarasan, D. Rajamani, and A. Renugambal, “*An approach on fuzzy and regression modeling for hard milling process*”. Applied Mechanics and Materials, vol. 813, pp. 498-504, 2015.